J Mol Model (2012) 18:4797–4810
DOI 10.1007/s00894-012-1481-5

ORIGINAL PAPER

Validation of computational approach to study monomer selectivity toward the template Gallic acid for rational molecularly imprinted polymer design

Sushma Pardeshi · Rajendra Patrikar · Rita Dhodapkar · Anupama Kumar

Received: 7 February 2012 / Accepted: 21 May 2012 / Published online: 15 June 2012

Abstract Gallic acid (GA) is important for pharmaceutical industries as an antioxidant. It also finds use in tanning, ink dyes and manufacturing of paper. Molecularly imprinted polymers (MIP), which are tailor made materials, can play an excellent role in separation of GA from complex matrices. Molecular recognition being the most important property of MIP, the present work proposes a methodology based on density functional theory (DFT) calculations for selection of suitable functional monomer for a rational design of MIP with a high binding capacity for GA. A virtual library of 18 functional monomers was created and screened for the template GA. The prepolymerization template-monomer complexes were optimized at B3LYP/6-31G(d) model chemistry and the changes in the Gibbs free energy (ΔG) due to complex formation were determined on the optimized structures. The monomer with the highest Gibbs free energy gain forms most stable complex with the template resulting in formation of more selective binding sites in the polymeric matrix in MIPs. This can lead to high binding capacity of MIP for GA. Amongst the 18 monomers, acrylic acid (AA) and acrylamide (AAm) gave the highest value of ΔG due to complex formation with GA. 4-vinyl pyridine (4-Vp) had intermediate value of ΔG while, methyl methacrylate (MMA) gave least value of ΔG due to complex formation with GA. Based on this study, the MIPs were synthesized and rebinding performance was evaluated using Langmuir-Freundlich model. The imprinting factor for AA and AAm based MIPs were 5.28 and 4.80 respectively, 4-Vp based MIP had imprinting factor of 2.59 while MMA based MIP exhibited an imprinting factor of 1.95. The experimental results were in good agreement with the computational predictions. The experimental data validated the DFT based computational approach.

Keywords Density functional theory · Gallic acid · Hydrogen bond · Molecularly imprinted polymer · Template-monomer interactions

S. Pardeshi · A. Kumar (✉)
Chemistry Department,
Visvesvaraya National Institute of Technology,
Nagpur 440010, India
e-mail: drkumaranupama@rediffmail.com

A. Kumar
e-mail: anupamakumar@chm.vnit.ac.in

R. Patrikar
Electronics & Communication Engineering Department,
Visvesvaraya National Institute of Technology,
Nagpur 440010, India

R. Dhodapkar (✉)
National Environmental Engineering Research Institute, [CSIR],
Nagpur 440020, India
e-mail: rs_dhodapkar@neeri.res.in

Introduction

Molecular imprinting is a procedure used to synthesize molecularly imprinted polymers (MIP) by the formation of a polymer network around a template molecule. A pre-polymerization complex is formed between the template and functional monomer by non-covalent approach which can exhibit several possible interactions, such as hydrogen bonds, hydrophobic interactions, van der Waals forces as well as electrostatic interactions. These interactions determine the spatial arrangement of monomers around the template. This spatial arrangement is then fixed by polymerization of monomers in presence of crosslinker. Removal of the template leaves a chemically and sterically complementary void (imprint) in the polymer network which is able to rebind

the template [1]. The high selectivity and stability of MIPs render them promising alternatives to enzymes, antibodies, and natural receptors for use in various applications. MIPs have been developed for a variety of applications including chromatography [2–4], solid-phase extraction (SPE) [5], enzyme catalysis [6] drug delivery matrices [7] and biomimetic sensors [8]. Molecular imprinting is an attractive method for extraction of wide range of chemical compounds and can serve a useful technique for extraction of antioxidants [9]. MIPs are robust, inexpensive and in many cases possess affinity and specificity that are suitable for industrial applications.

Although MIP synthesis is easy and inexpensive, the selection of the best precursors for polymer preparation is not trivial in practice. Generally, selection of the best precursors is based on the trial and error approach, which is a tedious and reagent consuming task. Some monomer selection strategies, such as mathematical formalism like Chemometrics [10] and experimental protocols like combinatorial methods [11] are reported in order to modify the tedious imprinting protocol. However, these methods suffer from one or other drawbacks. The technical difficulty of performing detailed thermodynamic calculations on a multi-component system like MIP makes Chemometrics approach difficult to implement. In the combinatorial screening approach, the amount of resources and time required is more. For example, to check a simple two-component combination of 100 monomers one has to synthesize and test more than 5000 polymers which is a very difficult task. This task will be further complicated by the possibility that these monomers could be used in monomer mixtures in different ratios [12, 13].

Over the years, the approach is focused on computational modeling [14]. The computational modeling for design of MIP is based on the prophetic statement of Nicholls et al. [15], i.e., the basis for the molecular memory of MIPs lies in the formation of template–functional monomer adducts in the pre-polymerization reaction mixture. The quantity and quality of molecularly imprinted polymer recognition sites is a direct function of the extent of the template-monomer interactions present in the prepolymerization mixture. This prepolymerization complex is transformed into active binding or recognition sites after polymerization and template extraction. More stable the pre-polymerization complex is, more selective the MIP. Hence, the choice of functional monomers capable of forming stable complexes with template is important.

Computational modeling considerably reduces the tedious task of finding the best recipes for MIPs. A number of studies are reported describing the application of computational methods for the design of molecularly imprinted polymers, which includes application of *ab initio* and semi-empirical methods to the design of MIPs [16]. Dong et al. [17] employed computational approach to screen monomers using the binding energy (ΔE) of the template theophylline and monomers as a measure of their interaction. Dineiro et al. [18] used the similar approach to select the best functional monomer and porogenic solvent for the template homovanillic acid for the creation of a sensor.

In the present study, the authors have reported the use of computational modeling for selection of optimal functional monomer for synthesis of Gallic acid (GA) based MIP. GA is an important antioxidant of polyphenol family. GA possesses scavenging activities against several radicals and protects cells from damage induced by UV-B or ionizing irradiation [19]. It is extensively used in tanning, ink dyes, as well as in the manufacturing of paper and also as an important substrate for the synthesis of propyl gallate in the food industry and the drug trimethoprim in the pharmaceutical industry [20]. GA is generally extracted from the natural matrix by conventional chromatographic methods which consume a large quantity of solvents [21]. Thus, development of a simple extraction procedure for GA is important. Use of MIP may serve as a promising technique to extract GA from complex matrices [22]. MIPs synthesized using 4-vinyl pyridine as monomer and its use for extraction of GA from herbs is reported [23]. However, the selection of monomer was based on the experimental protocol which involves a considerable amount of chemicals as well as tedious work involved in finding the best recipe for MIP.

In the past few years, Density Functional Theory (DFT) has emerged as a cost effective computational method in which, the effects of electron correlation is included. It is commonly applied to MIP studies due to the advantages such as high accuracy level of information, reliability, and reasonable computational costs in comparison with other computational methods [24]. The DFT method is also an established tool to study interactions such as hydrogen bonds [25].

The molecular modeling and simulation methods were used by Madhan et al. [26] to study the interaction between GA and collagen with the aim to study the stability of collagen brought about by the GA molecule in the process of tanning. Authors reported use of molecular mechanics and molecular dynamics to analyze interaction of GA with the collagen and binding of GA with peptide models in order to understand the effect of hydrogen bonding and non-covalent interactions. In continuation to this study, interaction energy of various dipeptides with GA was calculated using DFT and various modes of intermolecular complexation were explored [27].

In the present work, the functional monomer capable of forming most stable complex with the template GA is screened from a virtual library of 18 functional monomers

in order to synthesize the MIP which can selectively rebind the GA from the complex matrix. The template-monomer complexes were simulated and the change in the Gibbs free energy (ΔG) of the complex formation between the template and the functional monomers was computed for selection of an optimal functional monomer. To check the validity of the theoretical predictions, the MIPs were prepared with the functional monomers showing highest, average and least ΔG with GA. The rebinding capacity of MIPs was determined experimentally and their performance was compared with the theoretical binding score. To the best of our knowledge, this is the first report on the computational study of MIPs for GA with its experimental validation.

Materials and methods

Computational methods

Hardware and software

All computer simulations were undertaken on a workstation with an Intel Pentium 4, 3.20 GHz CPU, 4 GB RAM, and 260 GB hard disk running on the Linux operating system. The software employed in this work was Gaussian 03 [28] (Gaussian Inc., Wallingford, CT). Chem 3D Ultra 8.0.3 (Cambridgsoft Corporation, USA) provided graphical user interface for Gaussian.

Geometry optimization and energy computations

The designing of MIP includes several steps, mentioned as follows.

Building of models The first step was building of molecular models using Chem 3D Ultra software. The virtual library of functional monomers consisting of acidic, basic and neutral monomers is presented in Table 1.

The 3-D structures were drawn and cartesian coordinates of stable conformers were generated to prepare input file for running the Gaussian simulations.

Geometric optimization The B3LYP (Becke-Style 3-Parameter density functional theory using the Lee-Yang-Parr correlation function) with 6-31G(d) basis set was used for geometry optimizations to obtain structures with minimum energy.

Frequency calculations The harmonic vibrational frequencies confirmed the structures as minima with no imaginary frequencies and enabled the calculation of Gibbs free energies.

Calculation for change in the Gibbs free energy (ΔG) during the complex formation - The Gibbs free energy gains of the complexes were calculated using Eq. 1

$$\Delta G = G_{\text{template–monomer complex}} - [G_{\text{template}} + G_{\text{monomer}}] \quad (1)$$

where ΔG is the change in Gibbs free energy on the formation of template-monomer complex, $G_{\text{template–monomer complex}}$ is the Gibbs free energy of template-monomer complex, G_{template} is the Gibbs free energy of template and G_{monomer} is the Gibbs free energy of monomer molecules.

Chemicals

GA, acrylic acid (AA), 4-vinyl pyridine (4-Vp) and methyl methacrylate (MMA) were purchased from Sigma-Aldrich (Buchs, Switzerland). Ethylene glycol dimethacrylate (EGDMA), acrylamide (AAm) were purchased from Merck (Darmstadt, Germany), and 2,2-azoisobutyronitrile (AIBN) from National Chemicals (India). AIBN was recrystallized using methanol before use. All the solvents were reagent grade or HPLC-grade and purchased from Merck (India) and used without further purification.

Preparation of imprinted and non-imprinted polymers

The template GA, 0.17 g (1 mmol) and functional monomer AA, 0.28 g (4 mmol) were added into 10 mL acetonitrile in a round bottom flask, followed by 7.92 g of cross-linker EGDMA (40 mmol) and initiator AIBN (50 mg). This prepolymerization solution was sonicated for 15 minutes till all the precursors dissolved in the porogen. The mixture was cooled in ice and subsequently purged with nitrogen for five minutes to remove oxygen and other polymerization inhibitors. The flask was sealed and polymerization was performed via thermal initiation in a water bath maintained at 60 °C for 12 hours to obtain MIP_{AA}.

Similar procedure was followed using 0.28 g of AAm (4 mmol), 0.42 g of 4-Vp (4 mmol) and 0.33 g of MMA (4 mmol), as the functional monomers to obtain MIP_{AAm}, $MIP_{4\text{-}Vp}$ and MIP_{MMA} respectively. The resultant rigid bulk products were washed with water to remove the unreacted precursors, dried, crushed and ground into powder with mortar and pestle and passed through sieves (ASTM No. 200 and 240) to obtain particle size fractions between 63 and 75 μ. Retained particles (≥75 μ) were reground and passed through the sieve again. The remaining fine particles were removed by sedimentation in acetone. Non-imprinted polymers (NIP_{AA}, NIP_{AAm}, $NIP_{4\text{-}Vp}$, and NIP_{MMA}) were prepared following the same procedure as for the imprinted polymers but, without addition

Table 1 Virtual library of monomers created for screening with GA for preparation of MIPs

Functional Monomer	Optimized structure	Nature
Acrylamide	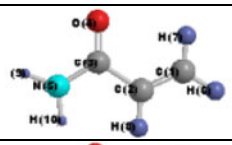	Neutral
Methacrylamide	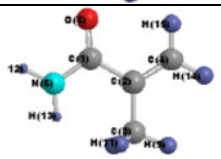	Neutral
Methyl methacrylate		Neutral
Acrylonitrile		Neutral
Hydroxy ethyl methacrylate	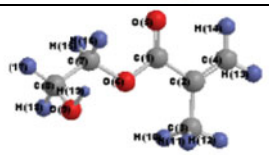	Neutral
Methacrylamido -glycolate	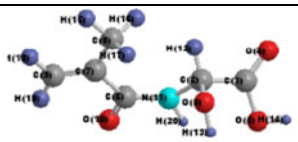	Neutral
Vinylglycine	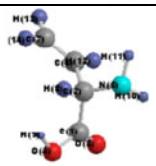	Neutral
Methacrylic acid	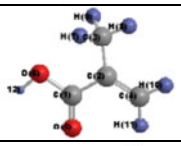	Acidic
Acrylic acid	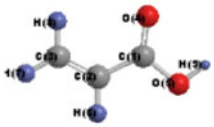	Acidic

of the print molecule (GA). NIPs were washed with water to remove the unreacted precursors followed by grinding and sieving.

The MIPs were washed with methanol:acetic acid (80:20 v/v) to extract GA from its polymeric matrix in a Soxhlet extractor. The procedure was repeated for subsequent cycles until no desorption of the template was observed in the eluent. After complete template removal, MIPs were washed with solution of 0.1 mmolL^{-1} Na_2CO_3 followed by water to remove the residual acetic acid. Finally, the polymers were dried at 55 °C for 6 hours and stored at ambient temperature for further experiments.

Table 1 (continued)

4-vinyl benzoic acid	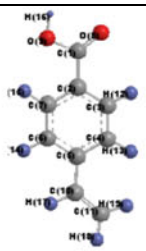	Acidic
Trifluoromethacrylic acid	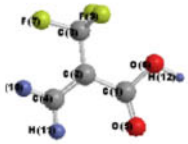	Acidic
Acrylamido-(2-methyl)-propane sulfonic acid		Acidic
3-Anilino-1-propanesulfonic acid	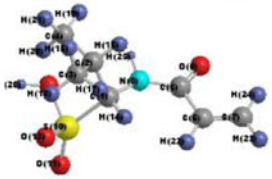	Acidic
4-Vinyl pyridine		Basic
2-Vinyl pyridine	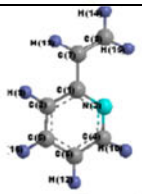	Basic
Allylamine		Basic
1-Vinyl imidazole		Amphoteric
4(5)-Vinyl imidazole	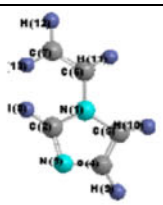	Amphoteric

UV-visible spectroscopy analysis

A series of prepolymerization complexes were prepared using a varying amount of monomers (0.08 $mmolL^{-1}$, 0.16 $mmolL^{-1}$, 0.24 $mmolL^{-1}$, 0.32 $mmolL^{-1}$) with a fixed amount of GA (0.08 $mmolL^{-1}$) in acetonitrile and their UV absorbance spectra were recorded using corresponding solution of functional-monomer in acetonitrile as blank.

Equilibrium binding experiments for study of sorption isotherms

The rebinding experiments were carried out in triplicate to study the binding capacity of MIPs. A series of GA standard solutions (1-20 $mmolL^{-1}$) were prepared in acetonitrile. 10 mL aliquots of each solution were mixed with 50 mg of the imprinted and non-imprinted polymers separately, in 100 mL conical flasks. These mixtures were shaken at 25± 5 °C on a water bath shaker for five hours. The solutions were centrifuged at 4500 rpm for four minutes and the supernatant was filtered into 10 mL volumetric flask and analyzed for GA by UV-visible spectrophotometer at 268 nm.

Results and discussion

Selection of optimal functional monomer for synthesis of MIP for GA

Values of the Gibbs free energy gains of the complexes (ΔG) are presented in Table 2.

From the values of Table 2, it was observed that three monomers namely acrylic acid, methacrylamidoglycolate and acrylamide formed the most stable complex with GA, amongst which acrylic acid was found to possess the strongest affinity for GA. The most striking observation is that, contrary to the usually applied criteria, an acidic functional monomer, AA, was found to be the best monomer for the imprinting of an acidic template molecule. The carboxylic functional group of acidic functional monomers is an excellent hydrogen bond donor acceptor group which can participate in the formation of hydrogen bonding interactions with the template [29]. Due to this property acidic functional monomers can be used for imprinting of acidic templates

4-vinyl pyridine had medium ΔG with GA and methyl methacrylate gave lowest ΔG with the template.

Template-monomer complex formation

The optimized structure of template GA is presented in Fig. 1.

Table 2 Change in the Gibbs free energy (ΔG) due to the complex formation between the template and the functional monomers

Template-monomer complex	Δ G ($kcalmol^{-1}$)
Gallic acid –Acrylic acid	−21.2
Gallic acid – Methacrylamidoglycolate	−20.1
Gallic acid-Acrylamide	−19.8
Gallic acid - Acrylamido-(2-methyl)-propanesulfonic acid	−11.4
Gallic acid -Methacrylamide	−10.6
Gallic acid -3-anilino-1-propanesulfonic acid	−10.1
Gallic acid –Methacrylic acid	−9.7
Gallic acid –Hydroxy ethyl methacrylate	−9.3
Gallic acid -1-vinyl imidazole	−9.1
Gallic acid -Allylamine	−8.7
Gallic acid -4(5)vinyl imidazole	−8.5
Gallic acid - 4-vinyl pyridine	−8.2
Gallic acid – Vinylglycine	−7.4
Gallic acid - 2-vinyl pyridine	−6.9
Gallic acid –Vinyl benzoic acid	−6.2
Gallic acid -Acrylonitrile	−5.4
Gallic acid – Trifluoromethacrylic acid	−4.2
Gallic acid –Methyl methacrylate	−3.4

The optimized structures of template-monomer complexes were analyzed further to determine the nature of interaction between functional monomer and the GA. The structures of the template-monomer complexes are presented in Fig. 2a, b and c.

In all the complexes, the functional group of monomer interacted with GA through its carboxylic group. In the case of acrylic acid, methacrylamidoglycolate, acrylamide, acrylamido-(2-methyl)-propane sulfonic acid and

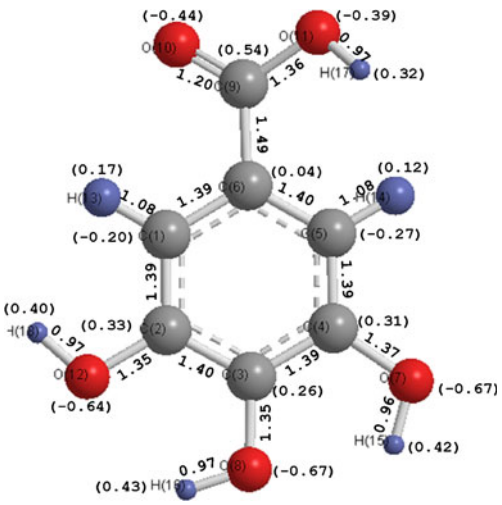

Fig. 1 Optimized structure of the template Gallic acid (GA) showing bond length between the various atoms, values in the bracket represents the atomic charge on atoms

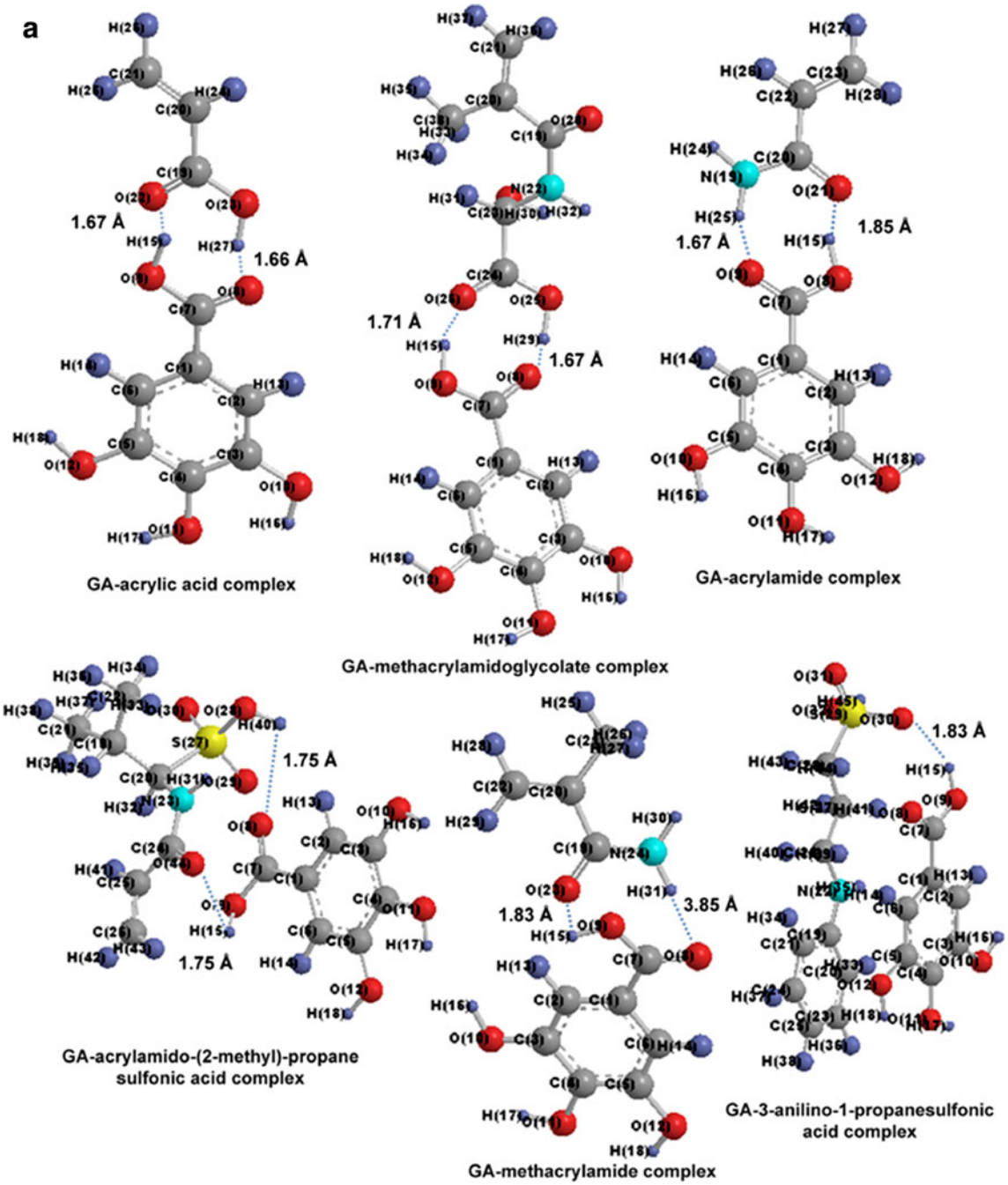

Fig. 2 **a**, **b** and **c** Optimized structures of prepolymerization complexes of GA generated at B3LYP/6-31G(d) model chemistry

methacrylamide complexes, two interactions were observed between the functional group of monomer and the hydrogen bond donor-acceptor –COOH group of GA.

The bonding distances for GA-acrylic acid complex was found to be 1.67 Å and 1.68 Å and it was the shortest amongst all the complexes. The bond distance for most of the complexes was found in the range of 1.8 Å. It was observed that as the bond distance increased, the value ΔG decreased.

Nature of interaction

Hydrogen bonds can be formed between proton donors such as N-H, O-H and proton acceptors such as C=O and are very important in imprinting [30]. It is well known that the hydrogen bond formation is related to the elongation of the proton donating R(X-H) bond due to shifting of proton to the other electronegative atom. Longer X-H bond leads to the shifting of proton to the other electronegative atom which in turn leads to stronger interaction between the two

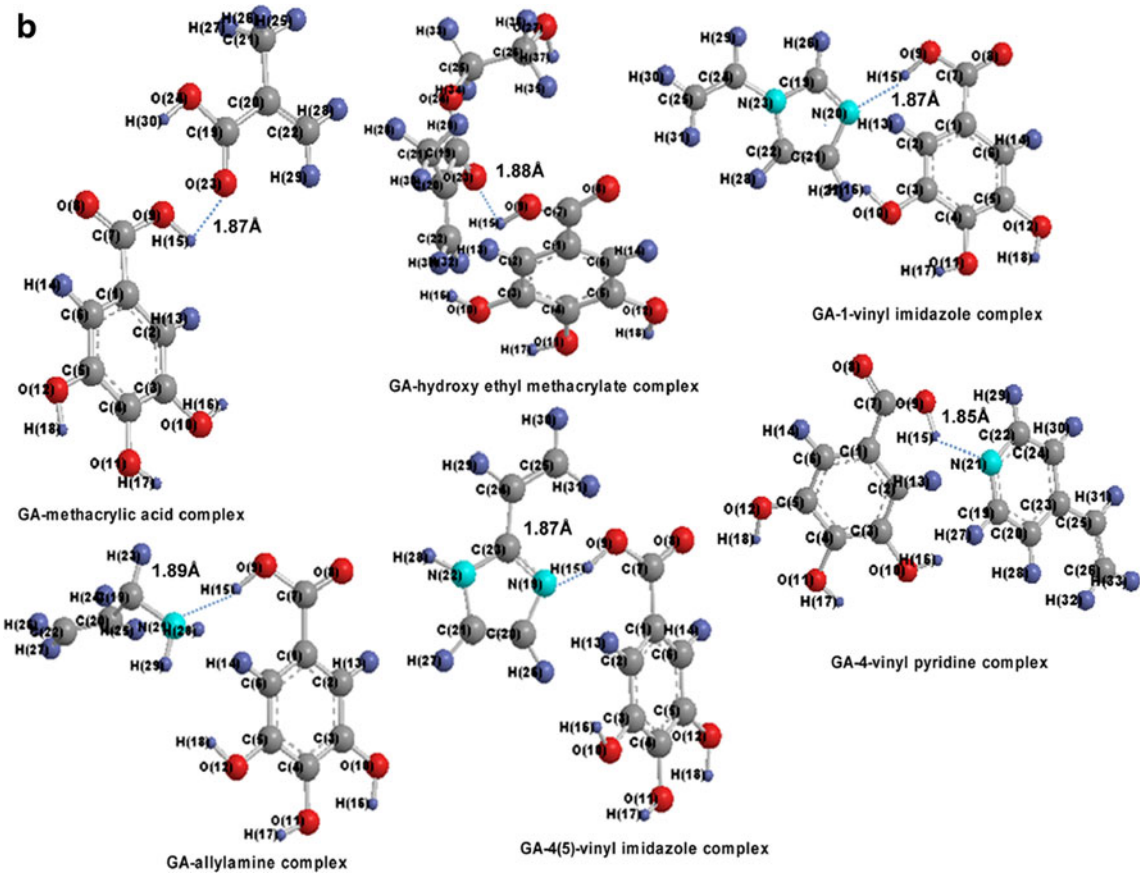

Fig. 2 (continued)

moieties involved in the hydrogen bonding [31]. Variation in bond length (ΔR) of the groups involved in the complex formation before and after complex formation were studied and reported in Table 3.

Analysis of complex geometries reveals that the distances of molecules such as R(O–H), R(C=O) and R(N-H) involved in bonding were elongated to some degree after formation of bonds between template and monomer as compared to isolated fragments. As shown in Table 3, most of the interactions had positive ΔR values. The highest value of ΔR (0.05 Å) was found in O9H15···O19=C22-bond of GA-acrylic acid complex.

Template-monomer complex mole ratio optimization

The computation time and cost increases with increase in the number of components in the model. In computational study of template-monomer interactions, the template-monomer complexes are simulated in 1:1 ratio in order to reduce computational cost and time required for simulation when a larger virtual library of monomers is tested with template. Further optimization of template-monomer mole ratio is carried out on the selected functional monomers [32, 33]. Following a similar approach, we studied the interaction energies of template GA with 18 different functional monomers. Further, mole ratio optimization of template-monomer complex was carried out in order to test the influence produced by the increase in the functional monomer concentration for the selected template-monomer complexes. The template-monomer complexes were simulated in the ratio from 1:1 to 1:6. The ΔG of template-monomer complexes with different mole ratio of monomer are presented in Table 4.

From Table 4 it can be seen that the ΔG values of template-monomer complex increased up to a ratio of 1:4 after that it decreased gradually for all the functional monomers. GA has four functional groups, one carboxylic which is a proton donor-acceptor group for hydrogen bond formation and three hydroxyl groups which act as donor sites for hydrogen bond formation. Consequently, four monomer molecules can participate in bond formation.

UV-visible spectroscopic analysis

UV-visible spectra of functional monomers, GA and template-monomer complexes in acetonitrile are presented in Fig. 3.

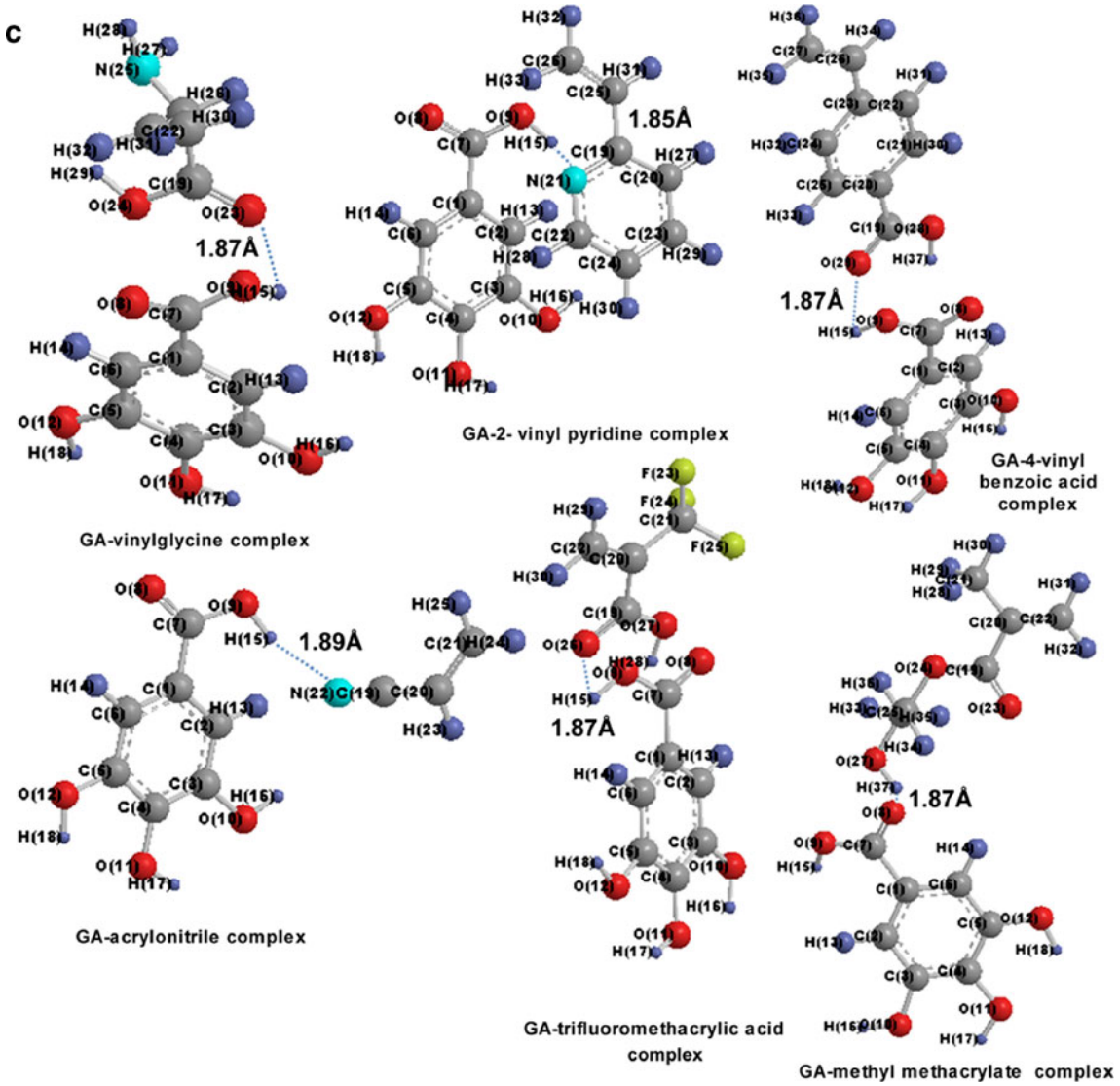

Fig. 2 (continued)

As shown in Fig. 3a, acrylic acid, acrylamide and methyl methacrylate have peaks at 194 nm, 198 nm and 205 nm respectively while 4-vinyl pyridine exhibits two absorption peaks at 197 and 241 respectively.

GA has two absorbance peaks at 214 nm and at 268 nm respectively (as seen in (1) of Fig. 3b, c, d and e). In the spectra of GA-AA complexes presented in Fig. 3b, the first absorbance peak of GA (at 214 nm) was red shifted with gradual decrease in the intensity. On moving from 1:0 to 1:4 molar ratio of template: monomer (from peak 1 to 5), the red shift ($\Delta\lambda$) was about 12.0 nm. The second peak of GA at 268 showed almost no shift in absorbance on addition of AA but its intensity considerably decreased.

Similarly, for GA-AAm and GA-MMA complexes presented in Fig. 3c and e, the peak of GA at 214 nm was slightly red shifted, with $\Delta\lambda$=3 nm for GA-AAm and $\Delta\lambda$=4 nm for GA-MMA respectively. Intensity of second peak of GA at 268 nm was decreased with no shift in absorbance wavelength for both complexes.

For GA-4Vp complex, presented in Fig. 3d intensity of both the peaks decreased with slight red shift ($\Delta\lambda$=3). The red-shift of the absorption band is typical for hydrogen bonding effect on the Л–Л* absorption band of a molecule whose chromophore acts as a proton donor. These observations indicate formation of hydrogen bonds between template and monomers [34].

Sorption isotherm and rebinding performance of polymers

To validate the computational modeling experiments, MIPs were prepared using monomers giving highest ΔG, i.e, acrylic acid and acrylamide, monomer with the average ΔG, i.e., 4-vinyl pyridine and the monomer with the least ΔG, i.e., methyl methacrylate with the template GA.

Table 3 Variations in the bond lengths of the groups involved in the formation of complex

Template-monomer complex	Bond parameters	$R_{Initial}$ (Å)	R_{T-M} (Å)	Δ R (Å) (R_{T-M} -$R_{Initial}$)
GA-Acrylic acid complex	i) R(O9-H15···O19=C22)			
	R(O9-H15)	0.97	1.02	0.05
	R(O19=C22)	1.21	1.24	0.03
	ii) R (C7=O8···H27-O23)			
	R(O23-H27)	0.97	1.00	0.03
	R(C7=O8)	1.20	1.23	0.03
GA-Methacrylamidoglycolate complex	i) (O9-H15···O26=C24)			
	R(O9-H15)	0.97	0.99	0.02
	R(O26=C24)	1.20	1.22	0.02
	ii) R (C7=O8···H29-O25)			
	R(H29-O25)	0.97	1.01	0.04
	R(C7=O8)	1.20	1.23	0.03
GA-Acrylamide complex	i) (O9-H15···O21=C20)			
	R(O9-H15)	0.97	1.00	0.03
	R(O21-C20)	1.22	1.24	0.02
	ii) (C7=O8···H25-N19)			
	R(C7=O8)	1.20	1.23	0.03
	R(N19-H25)	1.00	1.02	0.02
GA- Acrylamido-(2-methyl)-propane sulfonic acid complex	i) (O9-H15···O44=C24)			
	R(O9-H15)	0.97	0.99	0.02
	R(O44=C24)	1.20	1.24	0.04
	ii) (C7=O8···H40-O23)			
	R(C7=O8)	1.20	1.22	0.02
	R(H40-O23)	0.97	1.0	0.03
GA-Methacrylamide complex	i) (O9-H15···O23=C19)			
	R(O9-H15)	0.97	0.98	0.01
	R(O23=C19)	1.22	1.24	0.02
	ii) (C7=O8···H31-N24)			
	R(O8=C7)	1.20	1.21	0.01
	R(N24-H31)	1.00	1.01	0.01
GA-3-Anilino-1-propanesulfonic acid	(O9-H15···O30=C29)			
	R(O9-H15)	0.97	0.98	0.01
	R(O30=C29)	1.46	1.47	0.01
GA-Methacrylic acid complex	(O9-H15···O23=C19)			
	R(O9-H15)	0.97	0.98	0.01
	R(O23=C19)	1.21	1.23	0.01
GA-Hydroxy ethylmethacrylate	(O9-H15···O23=C19)			
	R(O9-H15)	0.97	0.98	0.01
	R(O23=C19)	1.21	1.22	0.01
GA-1-Vinyimidazole complex	(O9-H15···N20=C19)			
	R(O9-H15)	0.97	0.99	0.02
	R(N20=C19)	1.31	1.31	No change
GA-Allylamine complex	(O9-H15···N21-C19)			
	R(O9-H15)	0.97	0.99	0.02
	R(N21-C19)	1.47	1.47	No change
GA-4(5)Vinyimidazole complex	(O9-H15···N20=C19)			
	R(O9-H15)	0.97	0.99	0.02
	R(N20=C19)	1.37	1.37	No change

Table 3 (continued)

Template-monomer complex	Bond parameters	$R_{Initial}$ (Å)	R_{T-M} (Å)	Δ R (Å) (R_{T-M} -$R_{Initial}$)
GA-4-vinyl pyridine complex	(O9-H15···N21=C22)			
	O9-H15	0.97	0.99	0.02
	N21=C22	1.34	1.34	No change
GA-Vinylglycine complex	(O9-H15···O23=C19)			
	R(O9-H15)	0.97	0.97	No change
	R(O23=C19)	1.20	1.21	0.01
GA-2-vinyl pyridine complex	(O9-H15···N21=C22)			
	O9-H15	0.97	0.99	0.02
	N21=C22	1.33	1.33	No change
GA-4-Vinylbenzoic acid complex	(O9-H15···O29=C19)			
	R(O9-H15)	0.97	0.98	0.01
	R(O29=C19)	1.21	1.22	0.01
GA-Acrylonitrile complex	(O9-H15···N22-C19)			
	R(O9-H15)	0.97	0.97	No change
	R(N22-C19)	1.16	1.16	No change
GA-Triflouromethacrylic acid complex	(O9-H15···O26=C19)			
	R(O9-H15)	0.97	0.97	No change
	R(O26=C19)	1.21	1.22	0.01
GA-Methyl methacrylate complex	(O9-H15···O23=C19)			
	R(O9-H15)	0.97	0.98	0.01
	R(O23=C19)	1.21	1.22	0.01

Methacrylamidoglycolate was excluded from the study due to its commercial unavailability.

The rebinding isotherm models commonly applied to the MIPs are Langmuir isotherm, Freundlich isotherm and Langmuir-Freundlich (LF) model. However the most widely acceptable rebinding isotherm model is Langmuir-Freundlich (LF) model [35]. Not all imprinted polymers can be modeled using solely Freundlich or Langmuir isotherms. This is because; Langmuir isotherm and Freundlich isotherm are only accurate within limited concentration regions. The Langmuir isotherm best models the saturation behavior of an MIP, usually in the high concentration region whereas; the Freundlich isotherm is limited to the lower sub-saturation concentration region of the sorption isotherm. As MIPs improve, the concentration window that is measured will begin to span both saturation and sub saturation regions. In addition, to accurately characterize a system, the isotherm should be ideally measured over both concentration regions. Therefore these isotherms require hybrid heterogeneous binding models that can span both saturation and sub-saturation regions [36]. Along these lines, we have applied the Langmuir-Freundlich (LF) isotherm (Eq. 2) to characterize MIPs.

Table 4 ΔG of template-monomer complexes in different mole ratios of monomers in $kcalmol^{-1}$

Composition	ΔG ($kcalmol^{-1}$)			
	GA-AA	GA-AAm	GA-4Vp	GA-MMA
1:2	−25.2	−23.7	−9.8	−4.2
1:3	−30.8	−27.6	−13.3	−6.3
1:4	−36.4	−32.3	−16.5	−8.9
1:5	−32.1	30.4	−14.6	−7.5
1:6	−31.5	28.7	−12.8	−6.2

The LF model describes the relationship between the equilibrium concentration of absorbed (B) and free (F) analyte to characterize MIPs.

$$B = \frac{N_t a F^m}{(1 + aF^m)} \quad (2)$$

Where 'B' ($\mu molg^{-1}$) is the amount of analyte bound per unit weight of polymer, 'F' ($mmolL^{-1}$) is the concentration of analyte in solution at equilibrium, 'N_t' is the total number of binding sites, 'a' the distribution of binding sites of varying binding strengths present in the polymer and 'm' is the heterogeneity index. For a homogeneous material, $m=1$. When $m<1$, the material is heterogeneous [37]. The

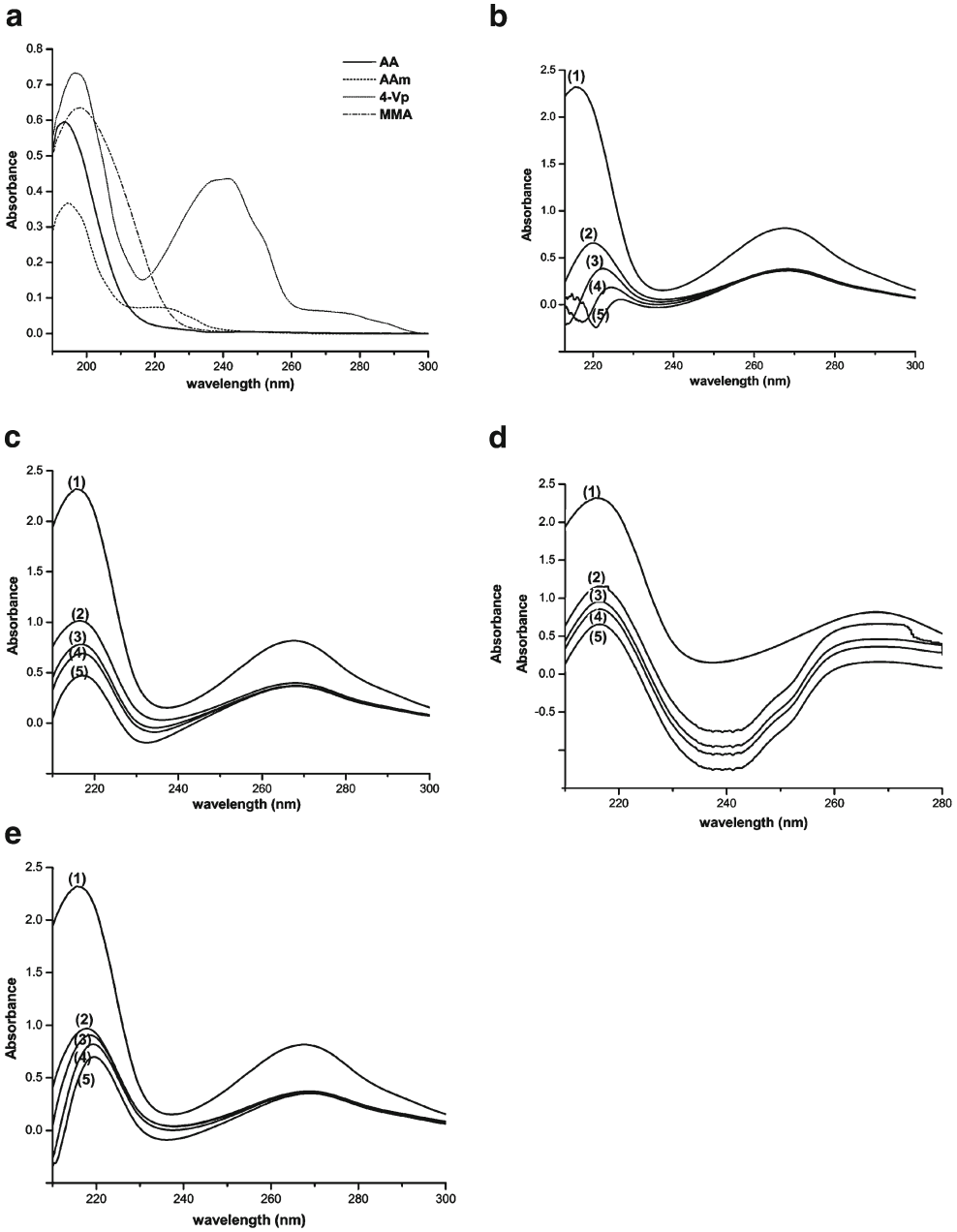

Fig. 3 UV spectra of (**a**) functional monomers, (**b**) GA in the presence of AA (**c**) GA in the presence of AAm, (**d**) GA in the presence of 4-Vp and (**e**) GA in the presence of MMA (concentration of GA (1)=0.08 $mmolL^{-1}$, concentration of monomers (1)=0 $mmolL^{-1}$, (2)=0.08 $mmolL^{-1}$, (3)=0.16 $mmolL^{-1}$, (4)=0.24 $mmolL^{-1}$ and (5)=0.32 $mmolL^{-1}$; corresponding solutions of pure monomers in acetonitrile were used as blanks)

rebinding performance of the MIP_{AA}, MIP_{AAm}, MIP_{4Vp} and MIP_{MAA} were studied using Langmuir-Freundlich (LF) model and the binding parameters were calculated to correlate the theoretical performance predicted in computational modeling and experimental data.

The imprinted and non-imprinted polymers were equilibrated with varying initial concentrations of GA in acetonitrile. The concentration of GA bound to polymers, i.e., binding capacity was plotted against concentration of GA in solution and rebinding isotherm data was fitted into the LF isotherm model. Equation 2 was used to fit the sorption isotherm by a non-linear least square-fitting program which yielded fitting parameters 'a', 'm' and 'N_t' as presented in Table 5.

From Table 5, it is observed that all the MIPs have an increased number of binding sites and have higher affinity distribution of binding sites (a) than the corresponding NIPs. The presence of template in the synthesis procedure creates the binding pockets of definite shape and selectivity in the MIPs [38].

It was observed that MIP_{AA} has the highest number of binding sites as well as a higher binding constant followed

by MIP_{AAm} and $MIP_{4\text{-}Vp}$. The values of N_t, a and K decreased for MIP_{MMA}.

The extent of template monomer interactions as the quantity and quality of molecularly imprinted polymer recognition sites is a direct function of the extent of the template-monomer interactions present in the prepolymerization mixture [15], thus the stability of the template-monomer complex (ΔG) can be correlated with the values of N_t.

The values of 'm' between 0 to 1 confirmed the existence of surface heterogeneity. The MIPs were more heterogeneous than the corresponding NIPs, due to the presence of varying types of binding sites in the MIPs. Significant trend of values of 'm' is not observed with the stability of the template-monomer complex strength as many factors such as process of polymerization and formation of different types of binding sites affects the surface heterogeneity [39] and no correlation of ΔG with surface heterogeneity is observed.

The specific rebinding in terms of the imprinting factor is presented in Fig. 4. The imprinting factor of MIP_{AA} was highest followed by MIP_{AAm} and $MIP_{4\text{-}Vp}$. The MIP_{MMA} had the lowest imprinting factor.

The rebinding performance of MIPs was in accordance with the trend of stability of the template-monomer complexes. Thus, it was found that computational predictions and experimental results were in good agreement based on the parameters of interaction energy of monomers and the rebinding performance of MIPs prepared using these monomers

Earlier reported value for the imprinting factor of GA based MIPs is 2.19 and 4-Vp was found to be a better monomer than AA when methanol was used as porogenic and rebinding solvent [23]. 4-Vinyl pyridine forms ionic interaction with GA and acrylamide forms hydrogen bonding interactions with the GA. Methanol is a polar protic solvent which can stabilize ionic interactions between 4-Vp and GA. On the other hand it disrupts hydrogen bond formation between acrylamide and GA which in turn leads to poor rebinding performance [40]. However, in the present study, acetonitrile an aprotic solvent is used as porogen and rebinding solvent which does not interfere with hydrogen bond formation.

The MIPs synthesized using the best monomer have shown an imprinting factor of 5.28. Thus, MIP with higher imprinting factor can be obtained using the functional monomer capable of forming a stable complex with GA. DFT based computational modeling proved useful for synthesizing MIPs with higher rebinding capacity and imprinting factor.

Table 5 Fitting parameters for Langmuir-Freundlich model for imprinted and non-imprinted polymers

Langmuir Freundlich model (LF)					
Polymer	N_t ($\mu molg^{-1}$)	a (M^{-1})	K ($mmol^{-1}$ L)	m	R^2
MIP_{AA}	512.85	63.09	98.13	0.7823	0.9921
NIP_{AA}	198.34	32.20	45.67	0.8947	0.9914
MIP_{AAm}	383.96	42.27	63.75	0.8564	0.9951
NIP_{AAm}	178.45	12.59	27.85	0.9522	0.9937
$MIP_{4\text{-}Vp}$	286.74	26.23	42.10	0.7864	0.9810
$NIP_{4\text{-}Vp}$	129.14	8.21	16.84	0.8874	0.9878
MIP_{MMA}	164.56	13.85	24.53	0.8612	0.9941
NIP_{MMA}	78.24	4.14	8.51	0.9567	0.9818

Conclusions

MIPs for GA were developed using quantum chemical computational approach. A virtual library of 18 functional monomers was developed and prepolymerization complexes were simulated using density functional theory. The simulated prepolymerization complexes indicated that the functional groups of monomer interacted with GA through its carboxylic acid group. Computational study predicted that AA is the most suitable functional monomer for synthesis of GA based MIP while MAA had the least ΔG with GA. The validation of the computational study as experimentally performed, was found in good agreement.

The rational computational MIP design is a safer and economical method in order to find the best monomer for a particular template before MIP synthesis. A large number of monomers can be tested against the template in a shorter span of time. By using the computational approach, it is possible to select the best monomer for MIP synthesis which in turn leads to better performance of MIP. This study proves useful in the selection of optimized MIP precursors for Gallic acid.

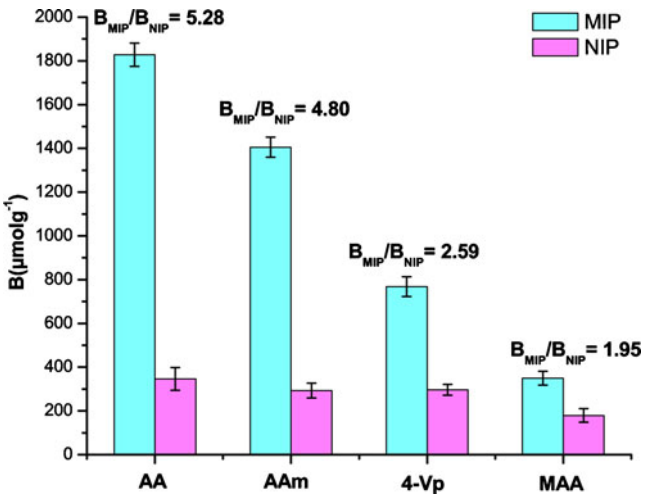

Fig. 4 Rebinding performance of MIPs in terms of imprinting factor

References

1. Verheyen E, Schillemans J, Wijk M, Demeniex M, Hennink W, Cornelus N (2011) Biomaterials 32:3008–3020
2. Feng Q, Zhao L, Yan W, Lin J, Zheng Z (2009) J Hazard Mater 167:282–288
3. Tsai W, Huang T, Huang J, Hsue Y, Chuang H (2009) J Chromatogr A 1216:2263–2269
4. Feng Q, Zhao L, Yana W, Lin J (2009) Anal Chim Acta 650:70–76
5. Yang M, Gu W, Sun L, Zhang F, Ling Y, Chu X, Wang D (2010) Talanta 81:156–161
6. Kirsch N, Dahlström J, Henschel H, Whitcombe M, Wikman S, Nicholls I (2009) J Mol Catal B: Enzym 58:110–117
7. Singh B, Chauhan N (2008) Acta Biomater 4:1244–1254
8. Mazzotta E, Malitesta C (2010) Sensors Actuators B 148:186–194
9. Pardeshi S, Kumar A, Dhodapkar R (2011) Mater Sci Forum 675–677:515–520
10. Davies M, Biasi V, Perrett D (2004) Anal Chim Acta 504:7–14
11. Díaz-García ME, Pina-Luis G, Rivero IA (2006) Trends Anal Chem 25:534–556
12. Karim K, Breton F, Rouillon R, Piletska E, Guerreiro A, Chianella I, Piletsky S (2005) Adv Drug Del Rev 57:1795–1808
13. Subrahmanyam S, Piletsky S (2009) In: Potyrailo R, Mirsky V (eds) Computational design of molecularly imprinted polymers, vol 1, Combinatorial methods for chemical and biological sensors. Springer, New York
14. Nicholls I, Andersson H, Charlton C, Henschel H, Karlsson B, Karlsson J, O'Mahony J, Rosengren A, Rosengren K, Wikman S (2009) Biosens Bioelectron 25:543–552
15. Nicholls I, Adbo K, Andersson S, Andersson P, Ankarloo J, Dahlström J, Jokela P, Jesper G, Karlsson A, Linus OA, Rosengren J, Shoravi S, Svenson J, Wikman S (2001) Anal Chim Acta 435:9–18
16. Azenha M, Kathirvel P, Nogueira P, Fernando-Silva A (2008) Biosens Bioelectron 23:1843–1849
17. Dong W, Yan M, Zhang M, Liu Z, Lin Y (2005) Anal Chim Acta 542:186–192
18. Diñeiro Y, Menéndez I, Blanco-López M, Lobo-Castañón M, Miranda-Ordieres A, Tunon-Blanco P (2006) Biosens Bioelectron 22:364–371
19. Kumagai J, Kawaura T, Miyazaki T, Prost M, Prost E, Watanabe M (2003) Radiat Phys Chem 66:17–25
20. Eslami A, Pasanphan W, Wagner B, Buettner G (2010) Chem Cen J 4:15–20
21. Lu J, Wei Y, Yuan Q (2007) Sepr Pur Tech 55:40–43
22. Kandimalla V, Ju H (2004) Anal Bioanal Chem 380:587–605
23. Zhu X, Cao Q, Yang X, Li F, Wang G, Ding Z (2009) Hel Chim Acta 92:78–87
24. Riahi S, Edris-Tabrizi F, Javanbakht M, Ganjali MR, Norouzi P (2009) J Mol Model 15:829–836
25. Zhang C, Hu J, Chen S, Fenglong J (2010) J Mol Model 16:1391–1399
26. Madhan B, Thanikaivelan P, Subramanian V, Rao J, Nair B, Ramasami T (2001) Chem Phys Lett 346:334–340
27. Madhan B, Parthasarathi R, Subramanian V, Rao J, Nair B, Ramasami T (2003) Chem Phys Lett 369:131–138
28. Frisch MJ et al. (2004) Gaussian, Inc. Wallingford, CT
29. Sellergren B (2001) Molecularly imprinted polymers: Man-made mimics of antibodies and their applications in analytical chemistry. Elsevier, Dordrecht
30. Komiyama M, Takeuchi T, Mukawa T, Asanuma H (2003) Molecular imprinting from fundamentals to applications. Wiley, Weinheim
31. Huang Z, Dai Y, Yu L, Wang H (2011) J Mol Model 17:2609–262
32. Khan M, Wate P, Krupadam R (2011) J Mol Model, article in press
33. Liu R, Li X, Li Y, Jin P, Qin W, Qi J (2009) Biosens Bioelectron 25:629–634
34. Joesern M, Schead L (1974) Hydrogen bonding. Marcel Dekker, New York
35. Pardeshi S, Kumar A, Dhodapkar R (2012) Adsorpt Sci Technol (in press)
36. Umpleby R, Baxter S, Chen Y, Shah R, Shimizu K (2001) Anal Chem 73:4584–4591
37. Ramstrom O (2005) Molecularly imprinted materials-science and technology. Dekker, New York
38. Rushton G, Karns C, Shimizu K (2005) Anal Chim Acta 528:107–113
39. García-Calźon J, Díaz-García ME (2007) Sensors Actuators B 123:1180–1194
40. Spivak D (2005) Adv Drug Deliv Rev 57:1779–1794